



CXCR4 Inhibition Counteracts Immunosuppressive Properties of Metastatic NSCLC Stem Cells

Orazio Fortunato¹, Dimas Carolina Belisario², Mara Compagno², Francesca Giovino¹, Cristiano Bracci^{2,3}, Ugo Pastorino⁴, Alberto Horenstein^{2,3}, Fabio Malavasi^{2,3}, Riccardo Ferracini⁵, Stefania Scala⁶, Gabriella Sozzi¹, Luca Roz^{1*}, Ilaria Roato^{2*} and Giulia Bertolini¹

¹ Tumor Genomics Unit, Fondazione Istituto di Ricovero e Cura a Carattere Scientifico (IRCCS) Nazionale dei Tumori, Milan, Italy, ² Center for Experimental Research and Medical Studies (CeRMS), Azienda Ospedaliera-Universitaria Città (AOU) della Salute e della Scienza di Torino, Turin, Italy, ³ Laboratory of Immunogenetics, Department of Medical Sciences, University of Turin, Turin, Italy, ⁴ Unit of Thoracic Surgery, Fondazione IRCCS Istituto Nazionale dei Tumori, Milan, Italy, ⁵ Department of Surgical Sciences (DISC), Orthopaedic Clinic-IRCCS, A.O.U. San Martino, Genoa, Italy, ⁶ Functional Genomics, Istituto Nazionale Tumori "Fondazione G. Pascale", IRCCS, Naples, Italy

OPEN ACCESS

Edited by:

Cristina MacCalli,
Sidra Medicine, Qatar

Reviewed by:

Claudia De Vitis,
Sapienza University, Italy
Jörg Wischhusen,
University Hospital Würzburg,
Germany

*Correspondence:

Luca Roz
luca.roz@istitutotumori.mi.it
Ilaria Roato
roato78@libero.it

Specialty section:

This article was submitted to
Cancer Immunity
and Immunotherapy,
a section of the journal
Frontiers in Immunology

Received: 21 March 2020

Accepted: 10 August 2020

Published: 02 October 2020

Citation:

Fortunato O, Belisario DC, Compagno M, Giovino F, Bracci C, Pastorino U, Horenstein A, Malavasi F, Ferracini R, Scala S, Sozzi G, Roz L, Roato I and Bertolini G (2020) CXCR4 Inhibition Counteracts Immunosuppressive Properties of Metastatic NSCLC Stem Cells. *Front. Immunol.* 11:02168. doi: 10.3389/fimmu.2020.02168

Cancer stem cells (CSCs) are functionally defined as the cell subset with greater potential to initiate and propagate tumors. Within the heterogeneous population of lung CSCs, we previously identified highly disseminating CD133+CXCR4+ cells able to initiate distant metastasis (metastasis initiating cells-MICs) and to resist conventional chemotherapy. The establishment of an immunosuppressive microenvironment by tumor cells is crucial to sustain and foster metastasis formation, and CSCs deeply interfere with immune responses against tumors. How lung MICs can elude and educate immune cells surveillance to efficiently complete the metastasis cascade is, however, currently unknown. We show here in primary tumors from non-small cell lung cancer (NSCLC) patients that MICs express higher levels of immunoregulatory molecules compared to tumor bulk, namely PD-L1 and CD73, an ectoenzyme that catalyzes the production of immunosuppressive adenosine, suggesting an enhanced ability of MICs to escape immune responses. To investigate *in vitro* the immunosuppressive ability of MICs, we derived lung spheroids from cultures of adherent lung cancer cell lines, showing enrichment in CD133+CXCR4+MICs, and increased expression of CD73 and CD38, an enzyme that also concurs in adenosine production. MICs-enriched spheroids release high levels of adenosine and express the immunosuppressive cytokine IL-10, undetectable in an adherent cell counterpart. To prevent dissemination of MICs, we tested peptide R, a novel CXCR4 inhibitor that effectively controls *in vitro* lung tumor cell migration/invasion. Notably, we observed a decreased expression of CD73, CD38, and IL-10 following CXCR4 inhibition. We also functionally proved that conditioned medium from MICs-enriched spheroids compared to adherent cells has an enhanced ability to suppress CD8+ T cell activity, increase Treg population, and induce the polarization of tumor-associated macrophages (TAMs), which participate in suppression of T cells. Treatment of spheroids with anti-CXCR4 rescued T cell cytotoxic activity and prevented TAM

polarization, likely by causing the decrease of adenosine and IL-10 production. Overall, we provide evidence that the subset of lung MICs shows high potential to escape immune control and that inhibition of CXCR4 can impair both MICs dissemination and their immunosuppressive activity, therefore potentially providing a novel therapeutic target in combination therapies to improve efficacy of NSCLC treatment.

Keywords: metastasis initiating cells, non-small cell lung cancer, CXCR4, immunosuppression, CD73, adenosine, tumor associated macrophage (TAM), PD-L1

INTRODUCTION

Lung cancer represents the first cause of cancer-related mortality worldwide (1). The predominant form of lung cancer is non-small cell lung cancer (NSCLC) for which available therapeutic options are largely ineffective because of its aggressiveness and diagnosis at metastatic phase (1). Treatment of NSCLC advanced stage disease used to rely on conventional platinum-based chemotherapy regimens that poorly impacted overall clinical outcome of patients, due to chemoresistance and frequent recurrence (2). Moreover, damage induced by chemotherapy in normal tissue has been proven to potentially cause the release of cytokines/chemokines that can sustain tumor cell survival and promote a receptive and immune-suppressive microenvironment able to chemoattract tumor cells at distant sites and foster metastasis initiation (3–5). Recently, immune checkpoint inhibitors (ICIs) have emerged as potentially revolutionary new drugs. First-line therapies combining cisplatin with ICIs may become the future mainstay of advanced NSCLC therapy (6–9). Unfortunately, a large number of patients still do not benefit from ICIs, and thus rationally designed combination strategies to extend ICIs effectiveness are mandatory (10).

We previously identified in NSCLC a subset of CD133+ lung cancer stem cells (CSCs), co-expressing CXCR4, endowed with stemness features and characterized by resistance to cisplatin and superior ability to seed distant site and initiate metastatic process (11–13).

CXCL12/CXCR4 axis has been described to play a pivotal role in CSCs maintenance, to guide tumor cell dissemination, and to foster chemoresistance (14–16). Cancer cells can up-regulate CXCR4 expression in response to extracellular adenosine, a potent immune suppressor molecule, thus acquiring increased ability to migrate and proliferate in response to CXCL12 (17, 18).

Due to its wide expression on several cell lineages, CXCR4 inhibition has been tested for different purposes and the CXCR4 inhibitor (Plerixafor) has been clinically approved for the mobilization of CD34+ hematopoietic stem cells for autologous transplantation in patients with lymphoma or multiple myeloma (19). Currently, several clinical studies are ongoing to test the efficacy of different CXCR4 inhibitors in metastatic patients with solid tumors (20–22). More recently, some studies have demonstrated that CXCR4 inhibition can reduce immunosuppression both by acting on Treg cells and myeloid derived suppressor cells (MDSC) that highly expressed CXCR4 receptor, overall resulting in the reactivation of T immune response against tumor cells (23–25).

CXCL12/CXCR4 axis synergizes with CD38 to support migration as a central step in tumor disease progression (26). CD38 is a pleiotropic glycoprotein receptor with enzyme activity involved in the catabolism of extracellular nucleotides (27). Therefore, multifunctional protein CD38 can contribute to immune suppressor of T cell, activating the non-canonical adenosinergic pathway that provides AMP substrate to CD73 (28, 29).

CD73 can be expressed on cancer cells and different immune cell populations. This molecule dephosphorylates extracellular adenosine monophosphate (AMP) generating free adenosine, which contributes to the immune-suppressive and pro-angiogenic microenvironment at the tumor site (30, 31). It is known that adenosine is involved in tumor immune escape, and thus the block of CD73 enzymatic activity can reactivate an antitumor immune response (32) by synergizing with chemotherapeutic drugs known to promote immunogenic responses and enhance the therapeutic activity of ICIs (33–35). Anti-CD73 antibody has been demonstrated effective in reducing tumor growth and metastatization in mice (32, 35, 36). Remarkably, CD73 expression has been described as a poor prognostic factor for overall survival in NSCLC (37). A significant population of CD39+CD73+ myeloid derived suppressor cells, capable of inhibiting T and NK cell activity, has been shown in peripheral blood and tumor tissues of NSCLC patients (38).

Immunotherapy based on ICIs have achieved significant results in clinical practice, improving survival of patients with cancer (39). However, only a fraction of patients have shown long-term benefit, and the high rate of resistance still limits their efficacy (40). The mechanisms of resistance to ICIs are quite different, and among them the up-regulation of CD38 by tumor cells determines a functional impairment of CD8 T cells, with a consequent tumor immune escape (41). Chen et al. demonstrated that the co-inhibition of immune checkpoints and adenosine release improves anti-tumor immune response (41).

Interestingly, also CXCR4 inhibition results effective in reverting tolerogenic polarization of tumor microenvironment (42) and in restoring sensitivity to CTLA-4 and PD-1 checkpoints inhibitors (24, 43).

Here, we report that NSCLC CD133+CXCR4+ metastasis-initiating cells (MICs) are endowed with immunosuppressive properties allowing them to escape immune control, by the expression of high levels of PD-L1 and CD73/CD38 ectoenzymes, that mediate extracellular adenosine generation (28). We prove the ability of a new class of CXCR4 antagonists (44) to counteract the immune suppressive behavior of metastatic NSCLC stem cells,

pointing at CXCR4 as novel target to prevent metastatic dissemination and immune escape mechanisms exploited by MICs.

MATERIALS AND METHODS

Cell Cultures and Pharmacological Treatments

NSCLC cell lines (A549, H1299, H3122, SW900) were purchased from ATCC and cultured in adhesion in conventional medium, RPMI-1640 supplemented with 10% heat-inactivated bovine serum (RPMI 10%) (FBS, all from Lonza). Bronchial-epithelial cells (HBEC3KT), immortalized by hTERT and CDK4, were obtained from Prof J. Minna (UT Southwestern) and cultured in Keratinocyte SFM (ThermoFisher).

To obtain sphere cultures, cells were plated in Ultra-Low Attachment plates (Corning) at a density of 10^4 cells/ml in serum-free medium DMEM/F12 (Lonza), supplemented with commercial hormone mix, B27 (Gibco), EGF 20 ng/ml, bFGF10 ng/ml (PeproTech), and heparin 2 µg/ml, named Stem Cells Medium (SCM). Floating sphere cultures were expanded for 15 days in the above medium. Once a week, they were gently dissociated with Accumax (Sigma-Aldrich) and re-plated as single cells in fresh medium.

Adherent cells and dissociated spheroids were incubated with peptide R 1 µM for 2 h at 37°C at a density of 2.5×10^5 cells/ml in respective complete medium. Next, the medium was removed and fresh medium was added and collected after 24 h to obtain cancer cell conditioned medium (CM).

PBMCs from healthy volunteers were plated at 1×10^6 cells/well in well plates and incubated at 37°C for 4 h. After the incubation, non adherent cells (T cells) were removed and used for the experiments. At the same time, adherent cells (monocytes) were differentiated to macrophages for 7 days with 50 ng/mL of human M-CSF.

Stimulation of T cells was performed by Dynabeads Human T-Activator CD3/CD28 and cultured in 50% of CM from different cancer cell lines. According to cell lines, negative control of the experiment were T cells cultured in RPMI 10% or 50% Stem Cell Medium (SCM).

Spheroids were treated with different concentration of mAb anti-CD73 (10, 20, 50 µg/ml, clone CB73, generated and purified in house through a two-steps HPLC chromatography by FM) or Adenosine 5'-(α,β -methylene)diphosphate (APCP, at 25, 50, 100 µM, Sigma) every 48 h for 7 days.

Flow Cytometry Analysis

To analyze tumor cell surface markers, single cell solution was washed in staining buffer (PBS1×+ 0.5% BSA+ 2mM EDTA) and incubated for 30 min at 4°C with the following antibodies: anti-human PE-CD133/1 (clone AC133/1Miltenyi Biotech), APC anti-human CXCR4 (44717 clone-R&D system), BB515 Anti-human CD73 (clone AD2), BB700 Mouse Anti-human CD38 (clone HIT2), BV421 Mouse Anti-human CD274 (PD-L1 clone MIH1), AlexaFluor488 Anti-Human HLA-ABC (clone DX17), and BV510 CD39 (clone A1) (all from BD Biosciences).

Primary tumor cell suspensions were obtained by digesting primary tumors, from consenting patients, with human Tumor Dissociation Kit (Miltenyi), subsequent filtering of dissociated tumor tissue on 100 µm pore cell strainer (Falcon), and erythrocytes removal by Red Blood Cell Lysis Solution (Miltenyi Biotech). Tumor cells were then stained with CD133, CXCR4, CD73, or PD-L1 (as specified above). Stromal cells were identified by staining for PE-Cy7 anti-human CD45, CD31, CD34 (eBioscience) and excluded by a negative gating strategy to perform tumor cell analysis.

To analyze the different subtypes of macrophages, cultured cells were washed in staining buffer and incubated for 30 min at 4°C with the following antibodies: Alexa488 anti-human CD206 (clone 15-2) (Biolegend) and PE anti-human CD163 (clone GHI/61) (Biolegend), APC anti-human CD14 (clone M5E2) (BD Biosciences).

For staining of T cytotoxic cells, lymphocytes were incubated in staining buffer with BV510 Anti-Human CD3 (HIT3a) and BB515 Anti-Human CD8 (clone Leu3a) for 30 min at 4°C; then the cells were fixed and permeabilized with BD Cytofix/Cytoperm™ Solution for 30 min at 4°C, washed in BD Perm/Wash buffer, and incubated with APC anti-human IFNγ (clone B27) (all from BD Bioscience), for 30 min at 4°C.

For analysis of Treg phenotype, T cells were first incubated with surface antibodies in staining buffer for 30 min at 4°C: BV510 Mouse Anti-Human CD3 (HIT3a), PE-Cy7 Anti-Human CD4 (clone Leu3a), APC Anti-Human CD25 (clone M-A251); then fixed and permeabilized with Transcription Factor Buffer Set, according to the datasheet instructions, and finally incubated with PE anti-Human FoxP3 (clone259D/C7) (all from BD Biosciences) for 30 min at 4°C. Tregs were identified within live cell gate as CD3+CD4+Foxp3+CD25^{high}.

For all analyses, dead cells were excluded by the use of Fixable Viability Stain 780 (BD Horizon). Data were acquired with a FACSCanto cytometer (BD) and analyzed by FlowJo software V10.

PBMCs Proliferation Assay

Two different tests were performed to assess T-cell proliferation: MTT and CFSE staining.

MTT assay: PBMCs derived from buffy coats were plated in a 96 well plate at 2×10^5 cells/well in RPMI, 10% FBS. To induce proliferation PBMCs were stimulated with OKT-3 (7.5 µg/ml) and anti-CD28 (7.5 µg/ml) and cultured with 50% of CM from cancer cells for 72 h.

MTT assay was performed according to the manufacturer's instructions (Sigma-Aldrich).

CFSE staining: T cells were incubated with CFSE (BD Biosciences) to a final concentration of 1.5 µM, for 8 min at room temp. The reaction was blocked by incubating cells in FBS. Stained T cell were plated at 1×10^5 cells/well in 24 well plates with RPMI+10% FBS and stimulated with antiCD3/CD8 microbeads and CM from tumor cells (ratio 1:1). Unstimulated T cells, plated in RPMI 10% or SCM +RPMI 10% (ratio 1:1) according to different tested CM, represent the negative control of the experiments. After 72 h T cells were analyzed by FACS to

assess the % of CFSE stained cells, which was inversely correlated to the proliferation rate.

Migration/Invasion Assay

For migration assays, 50,000 cells/well were incubated with peptide R inhibitor of CXCR4 (1 μ M) or AMD3100 (10 μ M) and seeded in 200 μ l of RPMI-1640 medium supplemented with 1% FBS onto 8 μ m-pore Transwell[®] cell culture inserts (BD Falcon) in 24 well plate. The lower chamber was filled with 500 μ l of RPMI supplemented with SDF-1 (50 ng/ml) as chemoattractant factor. For the invasion assay 1x10⁵ cells were plated onto 8 μ m-pore Transwell[®] cell culture inserts covered with 20 μ l of Matrigel, which was allowed to solidify at 37°C.

After 48 h (migration assay) or 72 h (invasion assay), cells on the top of the insert membranes were removed by gentle scraping with a sterile cotton swab while migrated/invaded cells in the lower side of the insert were fixed in methanol and mounted on slides using the VECTASHIELD Mounting Medium, containing DAPI. For each insert, cells in 4 random fields were counted by fluorescence microscope visualization at 20X magnification, and the values were averaged. Each experiment was performed in triplicate.

Adenosine Quantification

Twenty-four hours before the adenosine assay, adherent cells were seeded on 24 well plates at a concentration of 5 x 10⁵/500 μ L, while lung spheroid cells were transferred into 24 well plates in new medium, after have being cultured for 15 days (as previously described).

Culture medium was removed from adherent cells simply by pipetting, while spheroids cells were collected in Eppendorf tubes, centrifuged at low speed to pellet them down, and medium was removed. The cells and derived lung cancer spheroids were incubated with 100 μ L STOP solution (EHNA 100 μ mol/L, DYP 10 μ mol/L, and 10 μ mol/LDEF) (Sigma-Aldrich) for 15 min at 37°C and then treated with 100 μ L AMP 100 μ mol/L for 10 min at 37°C on a basculant. After incubation, the cells were collected in a tube containing acetonitrile (ACN; 1:2; 4°C), centrifuged (13000 g for 5 min at 4°C). Tubes were transferred into a Speed Vac (Eppendorf), to remove the supernatant, reconstituted in HPLC-grade water, and assayed or stocked at -80°C.

Chromatography analyses of the supernatant were performed with an HPLC (Beckman Coulter) fitted with a reverse-phase column (Synergi 4U Polar-RP80A; 150 x 4.6 mm; Phenomenex). Nucleotides and nucleosides were separated using a mobile-phase buffer (0.025 mol/L K₂HPO₄, 0.01 mol/L sodium citrate, 0.01 mol/L citric acid, adjusted with phosphoric acid to a pH of 5.1 and 8% acetonitrile (ACN) for 13 min at a flow rate of 0.6 mL/min. Ultraviolet (UV) absorption was measured at 254 nm. Chromatography-grade standards used to calibrate the signals were dissolved in PBS 1X, pH 7.4 (Sigma-Aldrich), 0.2 μ m-filtered, and injected in a volume of 15 μ L. The retention times (R_t, in min) of standards were: AMP, 5.8; inosine (INO), 6.4; and adenosine (ADO), 10; using a R_t window of \pm 5%. Peak area was calculated using Gold software (Beckman Coulter). Quantitative

measurements were inferred by comparing percentage area of each nucleotide and nucleoside analyzed, as previously described (29).

Real-Time PCR

Automating RNA isolation was performed by Maxwell RSC using simplyRNA Cells Kit (Promega). Expression levels of IL-10 and CD73 genes were determined by Real-Time PCR, using TaqMan[®] assays (Thermo Fisher) and normalized using the 2^{- $\Delta\Delta$ Ct} method relative to B2M, and results are expressed as mean \pm SD. For each PCR reaction, 5ng cDNA input was added.

Protein Extraction and Western Blot Analysis

Whole cell extracts were obtained from cell lines treated with 1 μ M CXCR4 inhibitor using GST-FISH buffer (10 mM MgCl₂, 150 mM NaCl, 1% NP-40, 2% Glycerol, 1 mM EDTA, 25 mM HEPES pH 7.5) supplemented with protease inhibitors (Roche), 1 mM phenylmethanesulfonylfluoride (PMSF), 10 mM NaF, and 1 mM Na₃VO₄. Extracts were cleared by centrifugation at 12,000 RPM for 15 min. The supernatants were collected and assayed for protein concentration using the Bio-Rad protein assay method. Twenty μ g of proteins were loaded on 12% Mini-PROTEIN TGX gels (BIO-RAD), transferred on nitrocellulose membrane (GE Healthcare), and blocked with 5% skim milk (BIO-RAD). Primary antibodies for immunoblotting included monoclonal anti-rabbit NT5E/CD73 (D7F9A clone, Cell Signaling Technology, CAT NO #13160) and rabbit polyclonal anti- β -actin (Sigma, CAT NO #A2066). Membranes were developed with ECL solution (GE Healthcare).

Statistical Analyses

Statistical analyses were performed using GraphPad Prism version 6.0. Statistically significant difference between two groups was assessed by two-sided Student's t-test. Statistical analyses among more than two groups was performed by one-way Anova with Tukey's *post hoc* test. Data are expressed as means and standard deviation, unless otherwise indicated. Statistical significance was defined as a P value less than 0.05.

RESULTS

Lung Cancer Metastasis Initiating Cells Highly Express PD-L1 and CD73 Markers

We initially investigated by flow cytometry the expression of PD-L1 and CD73 on surgically resected primary NSCLC samples (n=22), within tumor bulk population and CD133+ CSC subsets.

PD-L1 was significantly more expressed in CD133+ CSC subset (median value= 20%; min 2.5%, max 98%) compared to total population (median= 9.5%, min 0.5%, max 96%) (**Figure 1A**). Among CSC subsets, we could detect the population of mesenchymal CD133+EpCAM-CXCR4+ metastasis initiating cells (MICs) in 17 cases of primary tumors. Notably, we verified that it was the highest expressor of PD-L1 (median value= 31.8%; min 6%, max 100%). Conversely, CD133+ CSCs

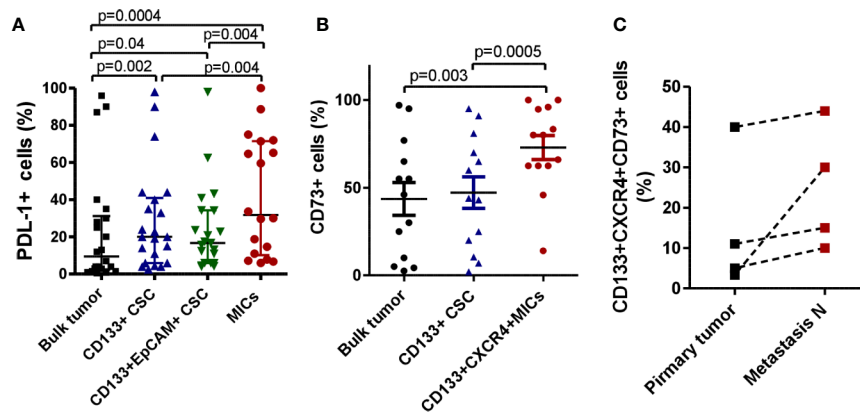


FIGURE 1 | MICs highly expressed immunoregulatory markers. **(A)** FACS analysis of N=22 NSCLC primary tumors. PD-L1 expression was assessed within bulk tumor population and different subsets of CD133+ Cancer Stem Cells, the epithelial one (EpCAM+) and the mesenchymal and metastatic one (CD133+CXCR4+ EpCAM- Metastasis initiating cells MICs). **(B)** FACS analysis of N=13 NSCLC primary tumors for the expression of CD73 within bulk tumor and different CSC subsets. **(C)** Comparison of CD73 expression by FACS analysis in n=4 primary tumors and synchronous lymph node metastases.

positive for the epithelial marker EpCAM showed lower expression of PD-L1 (median value = 16.6%; min 4%, max 98%) (**Figure 1A**).

We also observed a down-regulation of HLA class I, antigen presenting molecule, in CD133+ CSC compared to tumor bulk population, both in NSCLC primary tumors (n=6) and NSCLC cell lines (n=4) (0,7 fold decrease compared to bulk cells) (**Figures S1A, B**), confirming the ability of CSC to escape immune cells recognition. In 13 primary NSCLC samples, we also assessed CD73 expression within bulk population and CSC subsets. CD73 expression was significantly increased within the subset of CD133+CXCR4+ MICs (median value= 80%; min 14%, max 100%) compared to CD133+ CSCs (median= 44%; min 2%, max 95%) and bulk tumor (median= 46%; min 2.5%, max 65%) (**Figure 1B**).

Finally, in 4 cases, we were able to analyse primary tumors and corresponding synchronous lymph node metastases. The subset of metastatic and immunosuppressive CD133+CXCR4+ CD73+ MICs was 2.6 fold-enriched in metastasis compared to primary tumors (**Figure 1C**).

Overall, this immunophenotypic characterization of primary NSCLC indicates that CSCs and in particular the fraction of MICs displays high levels of molecules involved in immune suppression.

Lung Cancer Spheroids Are Enriched in MICs and Express Immunosuppressive Molecules

To study *in vitro* the immunosuppressive properties of MICs, we exploited a well-known method adopted to enrich for CSC population through the generation of cancer spheroids grown in selective medium, containing EGF and bFGF (45). We generated spheroids from 4 NSCLC cell lines: A549 and H3122 (adenocarcinoma), H1299 (large cell carcinoma), and SW900 (squamous cell carcinoma) (**Figure S2**). They were characterized

for CD133+CXCR4+ phenotype, PD-L1, HLA class I, and for CD73, CD38, and CD39 expression, involved in the production of immunosuppressive adenosine (29).

Overall, compared to their parental adherent cell lines, spheroids were highly enriched in CD133+CXCR4+ MICs subset (30 fold-change), generally associated with an increase of either CD73 or CD38 markers (respectively 1.2 and 3 fold-change), both involved in immune regulation and generation of adenosine (**Figure 2A**). The expression of CD39, the ectoenzyme that functions in tandem with CD73 in the canonical adenosinergic pathway, was undetectable both in adherent cells and spheroids, suggesting that in our *in vitro* condition CD38/CD73 non-canonical pathway is uniquely responsible for adenosine production.

Finally, no significant modulation of PD-L1 or HLA class I was observed in any spheroids cell lines compared to parental adherent one (data not shown). To address whether the increase in CD73/CD38 observed by flow cytometry analysis in CSC-enriched spheroids could be functionally associated with an increased production of ADO, we added AMP to adherent cells and sphere cultures and quantified adenosine production by HPLC. Results showed an increase of adenosine levels in medium from spheroids compared to adherent cells (**Figure 2B**). These data suggested a direct connection between high membrane expression of CD73/CD38 and production of adenosine.

We also investigated the modulation of IL-10, a cytokine known to trigger immunosuppressive effects by inducing T reg and pro-tumorigenic macrophages. Gene expression Real-Time analysis showed that spheroids expressed different levels of IL-10, whereas in all tested adherent cell lines IL-10 expression was undetectable (**Figure 2C**).

Overall, our results show that spheroids generated *in vitro* can be exploited to investigate the immunosuppressive phenotype of MICs.

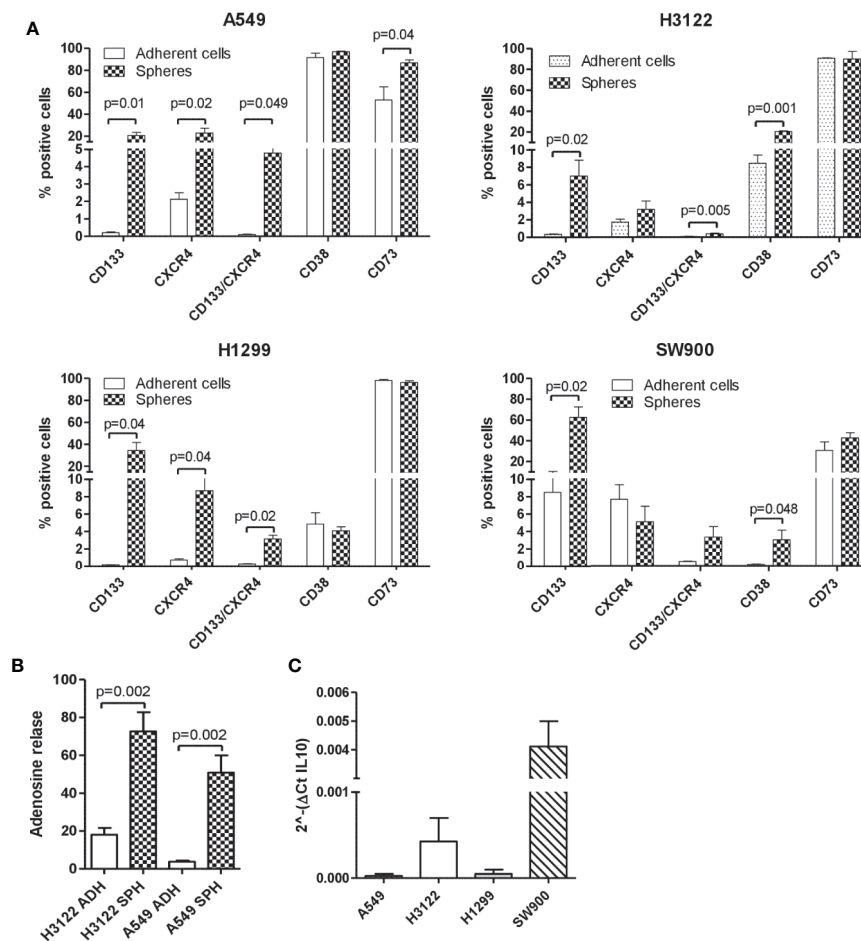


FIGURE 2 | Lung spheroids are enriched in MICs and expressed high level of immunosuppressive markers than adherent cells. **(A)** FACS analysis of adherent NSCLC cell lines (A549, H3122, H1299, SW900) and corresponding spheroids for expression of CD133, CXCR4, CD38, and CD73 markers. Data are the mean value \pm SD of n=4 analyses for each cell line. **(B)** AMP substrate was added to culture medium and generation of adenosine was quantified by HPLC in the medium of spheroids and adherent cells (A549 and H3122 cell lines). Data are the mean value \pm SD of n=2 analyses for each cell line. **(C)** IL-10 gene expression evaluated by Real-Time PCR in lung spheroids cultures. Bar are the mean value \pm SD of $2^{-\Delta\Delta CT}$ (IL-10-CT B2m).

Inhibition of CXCR4 Pathway Prevents Tumor Dissemination and Reduces Expression of Immunosuppressive Molecules

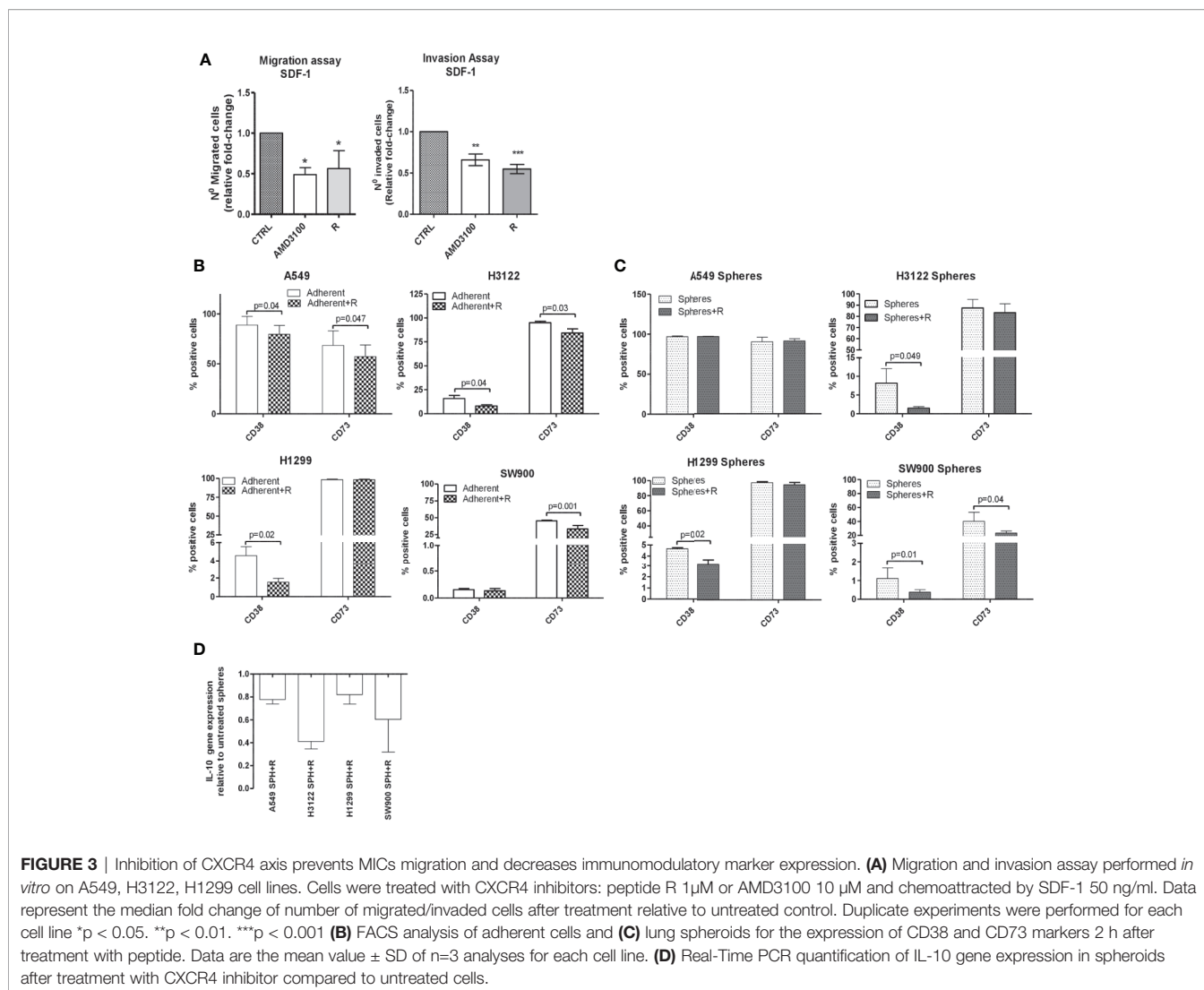
To block migration of CD133+CXCR4+ MICs, we tested a novel peptide inhibitor of CXCR4, peptide R, an analogue of SDF-1 (44).

Firstly, we assessed the ability of peptide R (1 μ M) to prevent both migration/invasion induced by SDF-1, similarly to AMD3100, a CXCR4 antagonist that has been clinically approved (**Figure 3A**). The experiments were performed in our panel of lung cancer cell lines.

We analyzed the phenotype of adherent cell lines after treatment with peptide R. Notably, we observed a reduced expression of markers, such as CD38 and CD73 (**Figure 3B**). We verified that the modulation of CD38 and CD73 expression induced by CXCR4 blockade was a rapid event, with the greatest

effect observed 2 h post treatment and that rapidly reverted to basal expression (**Figure S1A**). We also confirmed the down-regulation of CD73 after CXCR4 inhibition by WB and Real-Time analyses (**Figures S3B, C**).

However, since in adherent cell lines only a small percentage of cells expressed CXCR4 (median value 1.2%; min 0.7%, max 4.8%), we speculated that in lung cancer spheroids, highly enriched for CXCR4+ cells (median value 7.5%; min 2%, max 31.6%), treatment with peptide R might result in a more marked effect. Indeed, we proved that short-term treatment of spheroids with CXCR4 inhibitor was able to significantly reduce the expression of CD38 and/or CD73 in all cell lines (except for A549), likely indicating an adenosine decrease, and average 50% decrease of immunosuppressive IL-10 cytokine expression in all cell lines (**Figures 3C, D**). These results suggest a link between CXCR4 pathway and induction of immunosuppressive phenotype in MICs.



CXCR4 Axis Inhibition Partially Rescues T Cells Suppression Caused by MICs

To functionally prove the relevance of effects on immunosuppressive molecules modulation induced by CXCR4 inhibition, we tested the ability of CM collected from treated cell lines versus untreated controls, in both adherent and spheroids condition, to induce T cell suppression.

Firstly, we assessed the effects of CM from adherent cells and spheroids in modulating T cells having regulatory function (T reg: CD4+Foxp3+CD25^{high}). T cells from healthy volunteers were stimulated with anti CD3/CD28 micro beads and cultured in presence of CM from cancer cell lines. We showed that spheroids CM were able to increase the percentage of T reg compared to control, at higher extent than adherent cells (respectively 1.6 and 1.3 fold-increase). Notably, blockade of CXCR4 in both adherent and spheroid cells was sufficient to prevent the increase of T reg population induced by untreated counterpart (**Figure 4A**).

Next, since MIC-enriched spheroids were able to induce T reg phenotype, we assessed their potential to suppress T-cell activity. We demonstrated that lung spheroid CM were able to significantly suppress the proliferation of T cells, isolated from healthy donors PBMCs, after stimulation with anti CD3/CD28 antibodies (**Figure 4B**). When we compared the effect of spheroids and adherent cells, we observed that T cells from healthy donors proliferated significantly less in the presence of spheroids CM than adherent cells CM, and importantly, CM from spheroids treated with peptide R partially counteracted the suppressive effect on T cells (**Figure 4C**).

Finally, we verified that CM from spheroids were able to partially suppress (0.8 fold-change) the release of IFN- γ from CD8+ T cytotoxic cells (**Figure 4D**), derived from PBMCs of healthy volunteers, whereas CM from adherent cancer cell lines did not. CM from adherent and spheroid cancer cell lines treated with peptide R were able to relieve suppression of T cells and increase the subset of CD8+ T cells expressing IFN- γ compared to untreated cells (**Figure 4D**).

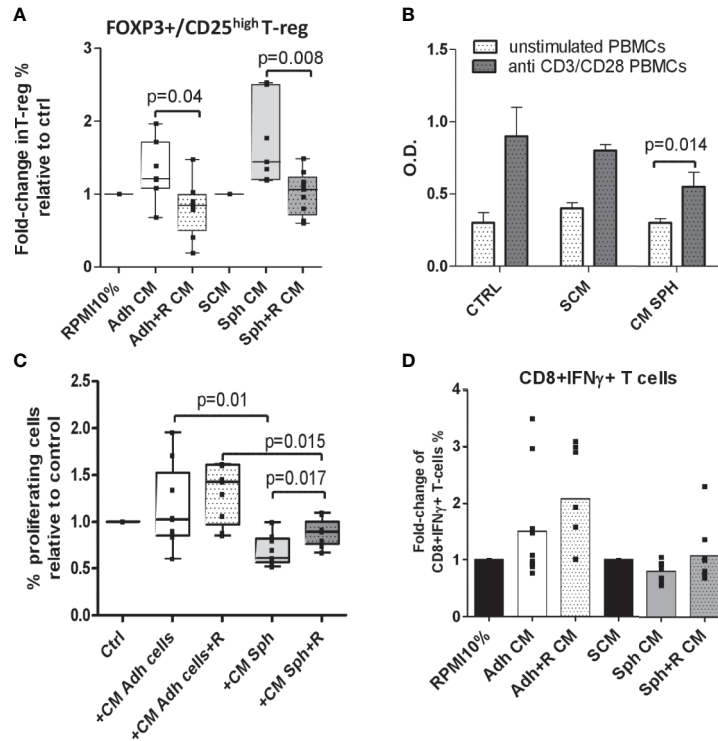


FIGURE 4 | CM from spheroids induces T cells suppression that can be prevented by CXCR4 inhibition. **(A)** FACS analysis for Treg population within T lymphocytes, from N=8 healthy volunteers. T lymphocytes were stimulated with anti CD3/CD28 beads and incubated for 72 h with CM from adherent or spheroids cell lines, untreated or treated with peptide R. Data are the fold-change in % T reg population compared to proper control medium (RPMI 10% for adherent cells and Stem cells medium- SCM- for spheroids). Data are the mean value \pm SD. N=2 independent experiments were performed for each tested NSCLC cell lines (A549/H3122/H1299/Sw900). **(B)** MTT assay measuring the proliferation of healthy volunteer T cells, unstimulated or stimulated with anti-CD3 and anti-CD28 antibodies, after exposure for 72 h to CM from A549 and H3122 spheroids or control RPMI or SCM medium for 72 h. Data are the mean value \pm SD of N=4 independent experiment for each cell line. **(C)** CFSE assay measuring proliferation of healthy volunteers T cells, stimulated with anti-CD3 and anti-CD28 microbeads, after exposure for 72 h to CM from adherent or spheroids, treated or not with peptide R. Data are the fold-change in % of proliferating cells compared to proper control medium (RPMI 10% for adherent cells and SCM for spheroid). Data are the mean value \pm SE of each NSCLC cell line (A549/H3122/H1299/SW900) tested in triplicate experiment. **(D)** FACS analysis for CD8+ T cytotoxic cells expressing IFN γ in N=8 healthy volunteers incubated for 72 h with CM from adherent or spheroids cell lines, untreated or treated with peptide R. Data are the fold-change in % CD8+ T cytotoxic population compared to proper control medium (RPMI 10% for adherent cells and Stem cells medium- SCM- for spheroids). Data are the mean value \pm SE of N=2 independent experiments were performed for each tested NSCLC cell lines.

Overall, our data functionally prove that spheroids enriched in MICs possess an enhanced ability to suppress T-cell activity, concomitantly with the above reported increase in adenosine and IL-10 production. CXCR4 blockade is able to impair MIC immune suppression activity, preventing T reg generation and rescuing T cell activity.

CXCR4 Inhibition Impairs CSC Ability to Promote TAM Polarization

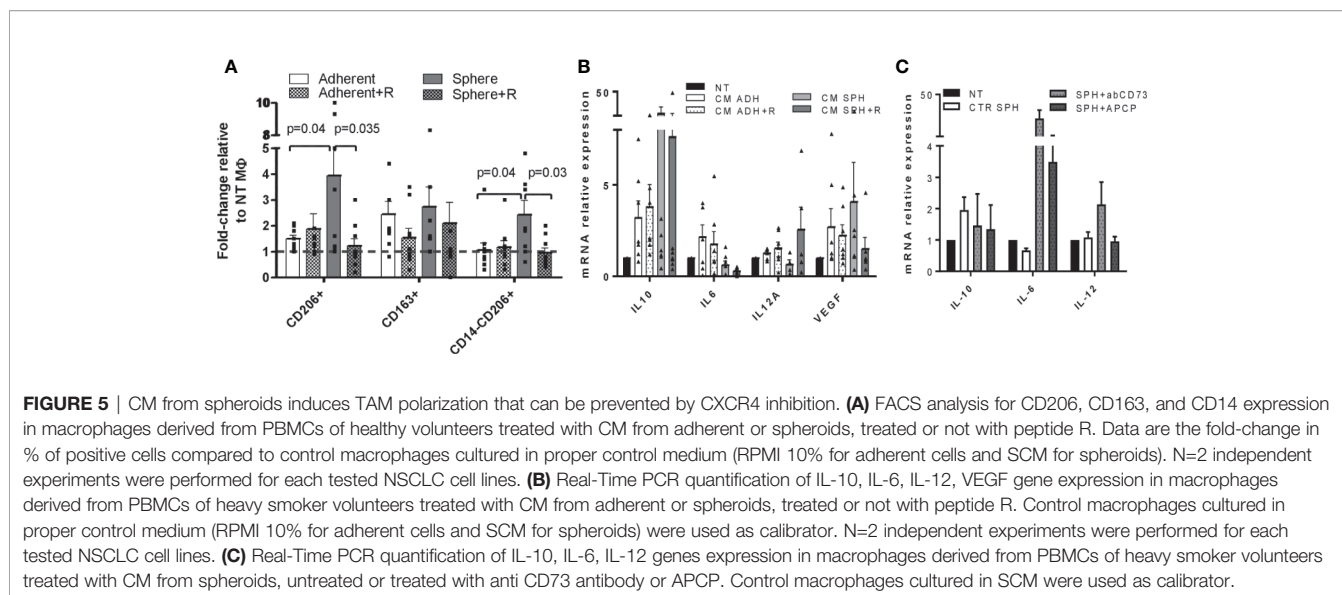
Finally, we tested the ability of CM from lung cancer cell lines treated or not with peptide R to induce M0 macrophages polarization toward tumor-associated macrophages (TAM), known to possess immunosuppressive properties (46).

Macrophage cultures were derived from healthy volunteers. We evaluated by FACS the increased percentage of CD206+, CD163+, and CD14-CD206+ cell subsets and by Real-Time PCR

an increased expression of IL-10, VEGF, and, conversely, a decreased expression of pro-inflammatory cytokines IL-12 and IL-6 as a read out of the induction of TAM phenotype after exposure to cancer cells CM, as reported by Benner et al. (47).

Despite the variability across macrophage cultures from different volunteers, we found that CM from spheroid cell lines enriched in MICs were more prone to induced TAM polarization compared to adherent cell lines, confirming the immunosuppressive behavior of MICs (**Figures 5A, B**). Indeed, CM from spheroids proficiently expanded the subset of CD206+/CD163+ and CD14-CD206+ macrophages (**Figure 5A**) and induced the up-regulation of IL-10 and VEGF with a concomitant decrease of IL-12 and IL-6 (**Figure 5B**), a phenotype typically associated with TAM.

To exclude that different medium composition (RPMI 10% or SCM) could drive modulation of immune regulation induced by cancer cells, we treated macrophage cultures with both RPMI



10% or SCM media conditioned by adherent NSCLC cell lines. We verified that the effects of the two CMs in the induction of TAM phenotype were very similar, indicating that different medium composition does not modify the intrinsic ability of cancer cells to induce TAM polarization (**Figure S4A**).

Finally, we assessed whether the observed increased immunosuppressive effects of spheroids reflect specific properties of selected cancer cells or can be related to the different *in vitro* culture conditions (adherent vs suspension). We exploited the immortalized but not tumorigenic human bronchial epithelial cell line (HBEC3-KT) that is not expected to induce an immunosuppressive effect on PBMCs. HBEC cells were grown in adhesion and in suspension as spheroids and SCM conditioned medium was collected by both cultures. Macrophages treated with SCM-CMs from both adherent and spheroids HBEC failed to show TAM polarization, as assessed by FACS and Real-Time PCR analyses (**Figure S4B**).

Overall, these data confirm that differences observed between CM from adherent and spheroids NSCLC cell lines are not due to medium composition or different culture conditions, but instead related to the intrinsic properties of spheres enriched in MIC population, with higher potential to induce immunosuppressive effects.

The treatment of lung spheroid cultures with peptide R was able to partially prevent TAM polarization, significantly reducing CD206/CD163 surface expression and IL-10, VEGF gene expression while increasing IL-12 production compared to untreated control (**Figures 5A, B**).

To prove the role of adenosine as a key mediator of immunosuppressive properties of MICs, we treated spheroids with the Adenosine 5²-(α,β -methylene)diphosphate (APCP) and with a neutralizing antibody against CD73, both able to impair adenosine production (29, 32). We observed that collected media from Ab-treated cells were able to revert TAM phenotype induced by lung cancer spheroids as indicated by a decrease of IL-10 and an increase of IL-6 and IL-12 (the latter was observed only after moAb treatment) (**Figure 5C**).

Overall, our data suggest that MICs-enriched spheroids not only directly act on T cell regulation but also induce polarization of TAM, which can exacerbate an immune suppressive environment.

DISCUSSION

Cancer stem cells are composed of heterogeneous populations, each with a specific function (48, 49). The subset of CSCs deputed to metastasis initiation possesses features allowing primary tumor escape, survival in circulation, and distant organs seeding (50, 51). Immune escape mechanisms adopted by MICs are supposed to be essential to complete all the steps leading to metastasis generation (52, 53).

Some evidence has reported that CSCs are characterized by specific immunological properties, which protect them against chemotherapeutic drugs but also increase their resistance toward apoptosis-inducing immune effectors, like T or NK cells (54). Several mechanisms can be exploited by CSCs to escape immune surveillance, such as down-regulation of MHC class I and II molecules, inefficient antigen presentation, and release of immunosuppressive factors (52). These strategies would help CSCs to survive, sustain tumor progression, and metastasize (53).

Moreover, it has been reported that there is a correlation between immunosuppressive environment and activation of epithelial to mesenchymal transition (EMT) program, endowing primary tumor cells with disseminating and stemness properties (52, 55). Dongre et al. showed that mesenchymal traits of tumor cells are associated with high levels of PD-L1 expression, content of T reg cells, and M2-like macrophages, proving that EMT activation in tumor cells promotes the recruitment of immunosuppressive cells and immune surveillance escape (56). In NSCLC the activation of EMT by the up-regulation of ZEB1 transcriptional factors causes the up-regulation of PD-L1 by tumor cells, leading to CD8⁺ T cells immune suppression and increased metastasis (57).

All together, these evidences suggest that a deeper understating of the immune profile of CSCs, and in particular of the mesenchymal subset deputed to metastasis initiation, can pave the way for specific anti-CSC immunotherapy, necessary to achieve a complete eradication of tumors and control of metastatic diseases.

In NSCLC, we previously showed that the population of CD133+/CXCR4+ MICs is endowed with stemness and EMT features, enhanced resistance to cisplatin, and superior ability to seed distant organs and initiate metastasis (11, 13). However, the immunological characterization of this subset has never been reported.

Here, we show that NSCLC MICs express the highest levels of both PD-L1 and CD73, compared to bulk tumor cells and epithelial CSC subset, suggestive for increased potential to suppress T cell activity.

An increased expression of PD-L1 has also been reported in CSCs of other tumor types. In head and neck carcinomas the subset of CD44+ CSCs expressing high level of PD-L1 can selectively evade host immune responses. The use of an immune check point inhibitor against PD-1 partially restored the immunogenicity of CD44+CSCs, providing the rationale for an anti CSC-immunotherapy (58).

In triple negative breast cancer, ALDH/CD44+ CSCs exhibited increased levels of PD-L1 versus non-CSC tumor cells. ALDH/CD44+/PD-L1+ CSCs were found in close contact with PD-1+ T cells both in murine and human tumor samples, suggesting a direct effect of CSCs in immune control (59).

In our study, we report that NSCLC CSCs co-expressing CXCR4 and CD73 are enriched in lymph node metastasis compared to primary tumors, indicating that the cells able to initiate metastasis may have an enhanced immunosuppressive activity.

This result confirms previously published literature reporting increased CD73 levels in metastatic tumors (31, 60). Moreover, studies deriving from different solid tumors reported CD73 expression as a poor prognostic factor (37, 61), suggesting that CD73-adenosine pathway plays a fundamental role in tumor dissemination, likely promoting immune suppression.

To investigate *in vitro* the immunosuppressive phenotype of CD133+/CXCR4+ CSCs overcoming the limitation of the paucity of CSCs in established adherent NSCLC cell lines, we adopted the sphere forming assay, a method commonly recognized to enrich for CSC subset (45). Spheroid cultures generated from NSCLC cell lines recapitulate the immunosuppressive phenotype of CD133+CXCR4+ MICs subset, also expressing higher levels of CD73 and CD38 as compared to adherent cells.

Adenosinergic signaling is a physiopathological regulator of tissue homeostasis, particularly upon injury and stress. Indeed, adenosine rapidly increases in response to stress, hypoxia, or tissue injury inducing repair processes (62). High levels of extracellular adenosine, generated by canonical CD39/CD73 or non-canonical CD38/CD73 adenosinergic pathways in tumor microenvironment (28, 29), can promote tumor progression by directly stimulating tumor proliferation, migration, invasion, and metastatic dissemination and by favoring immune escape of tumor cells

(33). From a functional point of view, CD133+CXCR4+ MICs subset showed an increased release of immunosuppressive adenosine, due to the activation of CD38/CD73 pathway, and indeed CD38 and CD73 resulted highly expressed, while CD39 expression was undetectable. Further, we also detected the increase release of IL-10, known to trigger immunosuppressive effects by inducing T reg cells and pro-tumorigenic immunosuppressive polarization of macrophages (63).

When we functionally tested *in vitro* immune regulatory properties of lung spheroids and corresponding adherent cells, we demonstrated that MICs-enriched spheroids possess an increased ability to induce T reg cells and consequently to suppress T cell proliferation as well as to reduce cytotoxic ability of CD8+ T cells.

Similarly, it was demonstrated that CSCs from glioblastoma inhibited T cell proliferation of healthy donors and showed lower immunogenicity and higher suppressive activity compared to corresponding adherent cell lines (64).

We also assessed the effect of spheroids to induce polarization of macrophages toward TAM phenotype that are very well known to promote immune suppression, tumor cell invasion, and metastasis (46, 65).

Conditioned media from cancer cells can be exploited to induce TAM polarization (47). In particular, TAM phenotype is associated with a high expression of immunosuppressive IL-10 and pro-angiogenic VEGF and low levels of inflammatory cytokines (IL-6 and 12). Besides, there is generally an increase of CD206/CD163 markers and reduced CD14 surface expression (47). All of these features were detected in cultures of macrophages derived from PBMCs of volunteers exposed to spheroids CM, thus *bona fide* providing support to the ability of MICs to induce TAM polarization that can exacerbate immunosuppressive environments.

It has been previously reported that one of the pathways stimulated by adenosine is the up-regulation of CXCR4 in cancer cells, increasing their ability to migrate and proliferate in response to CXCL12 (17). CXCR4 expression is an important factor for maintenance of stemness and endowment of metastatic potential of NSCLC CSCs (66). Thus, targeting CXCR4 could be useful both to block CSCs and to decrease tumor microenvironment immune suppression.

Moreover, CXCR4 is highly expressed also by the subset of immunosuppressive Treg cells. CXCR4 and its inhibition have been demonstrated in different tumor types to efficiently revert Treg suppression of T effectors proliferation, improving anticancer immune responses (23, 67).

CXCR4/CXCL12 axis inhibition has been demonstrated to revert tolerogenic polarization of tumor microenvironment (42) and to restore sensitivity to CTLA-4 and PD-1 ICIs (23, 43), overall representing a novel and effective way to counteract ICIs resistance. In the present study, we tested a novel peptide inhibitor of CXCR4, peptide R, analogue of CXCL12 (44), to target CD133+CXCR4+ MICs. We show that the treatment of NSCLC spheroids with Peptide R, besides preventing tumor cell dissemination, decreases expression of immunosuppressive molecules, such as CD73, CD38, and IL-10.

Furthermore, the functional blockade of CXCR4 in tumor cells is sufficient to prevent the immunosuppressive ability of MICs by restoring T cell proliferation and IFN γ expression, as well as partially preventing TAM polarization.

Our study has some limitations, mainly related to the small effects observed among treatment groups and the lack of *in vivo* validation of the findings. Indeed, treatment of PBMC with CM in some experiments resulted in biological effects that did not reach *statistical significance* mainly due to the great variability among PBMC from different healthy volunteers and to the use of several NSCLC cell lines. Despite the expected variability, we decided to test different NSCLC cell lines to take into consideration the heterogeneity of NSCLC histological subtypes and to avoid the potential bias of single cell line-dependent effects.

In vivo validation of our observation could definitely strengthen our conclusions. However, the *in vivo* investigation of the immunosuppressive ability of human tumor cells is hampered by the necessity to use immunocompromised mice, lacking adaptive immunity, to grow xenograft tumors. The establishment of a more sophisticated humanized murine model reconstituted with human immune cells might provide in the near future further validation of our *in vitro* evidence.

Finally, the validation of the potential of CXCR4 blockade to counteract MICs immune escape may be challenging *in vivo*. Since CXCR4 is widely expressed both by tumor and stroma/immune cells, the systemic delivery of CXCR4 inhibitors *in vivo* could affect these different cell subsets, impairing the possibility to finely dissect the players involved in the generation of the immunosuppressive microenvironment and the impact of CXCR4 inhibition on this tumor-stromal crosstalk.

Despite these limitations, taken together our data suggest the high ability of MICs to escape immune control and corroborate the link between CXCR4 pathway and the induction of immunosuppressive phenotype in CSCs. Consequently, they point at CXCR4 inhibitors as potential innovative agents to implement efficacy of immunotherapy, by concurring in reverting immune suppression and preventing metastatic dissemination.

REFERENCES

- Hirsch FR, Scagliotti GV, Mulshine JL, Kwon R, Curran WJ Jr., Wu YL, et al. Lung cancer: current therapies and new targeted treatments. *Lancet* (2016) 389:299–311. doi: 10.1016/S0140-6736(16)30958-8
- Chang A. Chemotherapy, chemoresistance and the changing treatment landscape for NSCLC. *Lung Cancer* (2011) 71:3–10. doi: 10.1016/j.lungcan.2010.08.022
- D'Alterio C, Scala S, Sozzi G, Roz L, Bertolini G. Paradoxical effects of chemotherapy on tumor relapse and metastasis promotion. *Semin Cancer Biol* (2019) 60:351–61. doi: 10.1016/j.semcancer.2019.08.019
- Karagiannis GS, Condeelis JS, Oktay MH. Chemotherapy-induced metastasis: mechanisms and translational opportunities. *Clin Exp Metastasis* (2018) 35:269–84. doi: 10.1007/s10585-017-9870-x
- Vyas D, Laput G, Vyas AK. Chemotherapy-enhanced inflammation may lead to the failure of therapy and metastasis. *Oncol Targets Ther* (2014) 7:1015–23. doi: 10.2147/OTT.S60114
- Reck M. Pembrolizumab as first-line therapy for metastatic non-small-cell lung cancer. *Immunotherapy* (2018) 10:93–105. doi: 10.2217/imt-2017-0121
- Herbst RS, Morgensztern D, Boshoff C. The biology and management of non-small cell lung cancer. *Nature* (2018) 553:446–54. doi: 10.1038/nature25183

DATA AVAILABILITY STATEMENT

All datasets presented in this study are included in the article/**Supplementary Material**.

ETHICS STATEMENT

The studies involving human participants were reviewed and approved by IRB of Fondazione IRCCS Istituto Nazionale dei Tumori. The patients/participants provided their written informed consent to participate in this study.

AUTHOR CONTRIBUTIONS

GB and IR conceived the study. OF, DB, FG, MC, CB, AH, IR, and GB performed the experiments and analyzed the data. LR, IR, and GB supervised data acquisition and analysis. UP provided clinical samples. SS provided the CXCR4 inhibitor. GB, IR, and OF wrote the manuscript. MC, AH, FM, RF, SS, GS, and LR reviewed and critically assessed the manuscript. All authors contributed to the article and approved the submitted version.

FUNDING

This work is supported by Associazione Italiana per la Ricerca sul Cancro (AIRC) (grant number IG21431 to LR and IG18812 to GS); Roche Italia (Roche per la Ricerca 2017 GB); CRT Foundation (CRT ordinary grant 2018 to IR).

SUPPLEMENTARY MATERIAL

The Supplementary Material for this article can be found online at: <https://www.frontiersin.org/articles/10.3389/fimmu.2020.02168/full#supplementary-material>

- Chatwal MS, Tanvetyanon T. Combination chemotherapy and immunotherapy in metastatic non-small cell lung cancer: a setback for personalized medicine? *Transl Lung Cancer Res* (2018) 7:S208–10. doi: 10.21037/tlcr.2018.07.15
- Giroux LE, Dumenil C, Julie C, Giraud V, Dumoulin J, Labrune S, et al. Immunotherapy revolutionises non-small-cell lung cancer therapy: Results, perspectives and new challenges. *Eur J Cancer* (2017) 78:16–23. doi: 10.1016/j.ejca.2016.12.041
- Pitt JM, Vetzizou M, Daillere R, Roberti MP, Yamazaki T, Routy B, et al. Resistance Mechanisms to Immune-Checkpoint Blockade in Cancer: Tumor-Intrinsic and -Extrinsic Factors. *Immunity* (2016) 44:1255–69. doi: 10.1016/j.immuni.2016.06.001
- Bertolini G, Roz L, Perego P, Tortoreto M, Fontanella E, Gatti L, et al. Highly tumorigenic lung cancer CD133+ cells display stem-like features and are spared by cisplatin treatment. *Proc Natl Acad Sci U S A* (2009) 106:16281–6. doi: 10.1073/pnas.0905653106
- Bertolini G, Gatti L, Roz L. The “stem” of chemoresistance. *Cell Cycle* (2010) 9:628–9. doi: 10.4161/cc.9.4.10821
- Bertolini G, D'Amico L, Moro M, Landoni E, Perego P, Miceli R, et al. Microenvironment-Modulated Metastatic CD133+/CXCR4+/EpCAM- Lung Cancer-Initiating Cells Sustain Tumor Dissemination and Correlate with

- Poor Prognosis. *Cancer Res* (2015) 75:3636–49. doi: 10.1158/0008-5472.CAN-14-3781
14. Scala S. Molecular Pathways: Targeting the CXCR4-CXCL12 Axis—Untapped Potential in the Tumor Microenvironment. *Clin Cancer Res* (2015) 21:4278–85. doi: 10.1158/1078-0432.CCR-14-0914
 15. Wang Z, Sun J, Feng Y, Tian X, Wang B, Zhou Y. Oncogenic roles and drug target of CXCR4/CXCL12 axis in lung cancer and cancer stem cell. *Tumour Biol* (2016) 37:8515–28. doi: 10.1007/s13277-016-5016-z
 16. Cojoc M, Peitzsch C, Trautmann F, Polishchuk L, Telegeev GD, Dubrovskaya A. Emerging targets in cancer management: role of the CXCL12/CXCR4 axis. *Onco Targets Ther* (2013) 6:1347–61. doi: 10.2147/OTT.S36109
 17. Richard CL, Tan EY, Blay J. Adenosine upregulates CXCR4 and enhances the proliferative and migratory responses of human carcinoma cells to CXCL12/SDF-1 α . *Int J Cancer* (2006) 119:2044–53. doi: 10.1002/ijc.22084
 18. Allard B, Turcotte M, Stagg J. CD73-generated adenosine: orchestrating the tumor-stroma interplay to promote cancer growth. *J BioMed Biotechnol* (2012) 2012:485156. doi: 10.1155/2012/485156
 19. Jantunen E. Novel strategies for blood stem cell mobilization: special focus on plerixafor. *Expert Opin Biol Ther* (2011) 11:1241–8. doi: 10.1517/14712598.2011.601737
 20. Porvasnik S, Sakamoto N, Kusmartsev S, Eruslanov E, Kim WJ, Cao W, et al. Effects of CXCR4 antagonist CTCE-9908 on prostate tumor growth. *Prostate* (2009) 69:1460–9. doi: 10.1002/pros.21008
 21. Huang EH, Singh B, Cristofanilli M, Gelovani J, Wei C, Vincent L, et al. A CXCR4 antagonist CTCE-9908 inhibits primary tumor growth and metastasis of breast cancer. *J Surg Res* (2009) 155:231–6. doi: 10.1016/j.jss.2008.06.044
 22. Richert MM, Vaidya KS, Mills CN, Wong D, Korz W, Hurst DR, et al. Inhibition of CXCR4 by CTCE-9908 inhibits breast cancer metastasis to lung and bone. *Oncol Rep* (2009) 21:761–7. doi: 10.3892/or_00000282
 23. Chen IX, Chauhan VP, Posada J, Ng MR, Wu MW, Adstamongkonkul P, et al. Blocking CXCR4 alleviates desmoplasia, increases T-lymphocyte infiltration, and improves immunotherapy in metastatic breast cancer. *Proc Natl Acad Sci U S A* (2019) 116:4558–66. doi: 10.1158/1538-7445.SABCS18-2744
 24. Zeng Y, Li B, Liang Y, Reeves PM, Qu X, Ran C, et al. Dual blockade of CXCL12-CXCR4 and PD-1/PD-L1 pathways prolongs survival of ovarian tumor-bearing mice by prevention of immunosuppression in the tumor microenvironment. *FASEB J* (2019) 33:6596–608. doi: 10.1096/fj.201802067RR
 25. Jiang K, Li J, Zhang J, Wang L, Zhang Q, Ge J, et al. SDF-1/CXCR4 axis facilitates myeloid-derived suppressor cells accumulation in osteosarcoma microenvironment and blunts the response to anti-PD-1 therapy. *Int Immunopharmacol* (2019) 75:105818. doi: 10.1016/j.intimp.2019.105818
 26. Vaisitti T, Aydin S, Rossi D, Cottino F, Bergui L, D'Arena G, et al. CD38 increases CXCL12-mediated signals and homing of chronic lymphocytic leukemia cells. *Leukemia* (2010) 24:958–69. doi: 10.1038/leu.2010.36
 27. Malavasi F, Deaglio S, Funaro A, Ferrero E, Horenstein AL, Ortolan E, et al. Evolution and function of the ADP ribosyl cyclase/CD38 gene family in physiology and pathology. *Physiol Rev* (2008) 88:841–86. doi: 10.1152/physrev.00035.2007
 28. Horenstein AL, Bracci C, Morandi F, Malavasi F. CD38 in Adenosinergic Pathways and Metabolic Re-programming in Human Multiple Myeloma Cells: In-tandem Insights From Basic Science to Therapy. *Front Immunol* (2019) 10:760. doi: 10.3389/fimmu.2019.00760
 29. Horenstein AL, Chillemi A, Zaccarello G, Bruzzone S, Quarona V, Zito A, et al. A CD38/CD203a/CD73 ectoenzymatic pathway independent of CD39 drives a novel adenosinergic loop in human T lymphocytes. *Oncoimmunology* (2013) 2:e26246. doi: 10.4161/onci.26246
 30. Allard D, Chrobak P, Allard B, Messaoudi N, Stagg J. Targeting the CD73-adenosine axis in immuno-oncology. *Immunol Lett* (2019) 205:31–9. doi: 10.1016/j.imlet.2018.05.001
 31. Jiang T, Xu X, Qiao M, Li X, Zhao C, Zhou F, et al. Comprehensive evaluation of NT5E/CD73 expression and its prognostic significance in distinct types of cancers. *BMC Cancer* (2018) 18:267. doi: 10.1186/s12885-018-4073-7
 32. Stagg J, Divisekera U, McLaughlin N, Sharkey J, Pommey S, Denoyer D, et al. Anti-CD73 antibody therapy inhibits breast tumor growth and metastasis. *Proc Natl Acad Sci U S A* (2010) 107:1547–52. doi: 10.1073/pnas.0908801107
 33. Allard B, Pommey S, Smyth MJ, Stagg J. Targeting CD73 enhances the antitumor activity of anti-PD-1 and anti-CTLA-4 mAbs. *Clin Cancer Res* (2013) 19:5626–35. doi: 10.1158/1078-0432.CCR-13-0545
 34. Allard B, Longhi MS, Robson SC, Stagg J. The ectonucleotidases CD39 and CD73: Novel checkpoint inhibitor targets. *Immunol Rev* (2017) 276:121–44. doi: 10.1111/immr.12528
 35. Young A, Ngo SF, Barkauskas DS, Sult E, Hay C, Blake SJ, et al. Co-inhibition of CD73 and A2AR Adenosine Signaling Improves Anti-tumor Immune Responses. *Cancer Cell* (2016) 30:391–403. doi: 10.1016/j.ccell.2016.06.025
 36. Terp MG, Olesen KA, Arnsperg EC, Lund RR, Lagerholm BC, Ditzel HJ, et al. Anti-human CD73 monoclonal antibody inhibits metastasis formation in human breast cancer by inducing clustering and internalization of CD73 expressed on the surface of cancer cells. *J Immunol* (2013) 191:4165–73. doi: 10.4049/jimmunol.1301274
 37. Inoue Y, Yoshimura K, Kurabe N, Kahyo T, Kawase A, Tanahashi M, et al. Prognostic impact of CD73 and A2A adenosine receptor expression in non-small-cell lung cancer. *Oncotarget* (2017) 8:8738–51. doi: 10.18632/oncotarget.14434
 38. Li J, Wang L, Chen X, Li L, Li Y, Ping Y, et al. CD39/CD73 upregulation on myeloid-derived suppressor cells via TGF-beta-mTOR-HIF-1 signaling in patients with non-small cell lung cancer. *Oncoimmunology* (2017) 6:e1320011. doi: 10.1080/2162402X.2017.1320011
 39. Chen L, Han X. Anti-PD-1/PD-L1 therapy of human cancer: past, present, and future. *J Clin Invest* (2015) 125:3384–91. doi: 10.1172/JCI80011
 40. Koyama S, Akbay EA, Li YY, Herter-Sprie GS, Buczkowski KA, Richards WG, et al. Adaptive resistance to therapeutic PD-1 blockade is associated with upregulation of alternative immune checkpoints. *Nat Commun* (2016) 7:10501. doi: 10.1038/ncomms10501
 41. Chen L, Diao L, Yang Y, Yi X, Rodriguez BL, Li Y, et al. CD38-Mediated Immunosuppression as a Mechanism of Tumor Cell Escape from PD-1/PD-L1 Blockade. *Cancer Discov* (2018) 8:1156–75. doi: 10.1158/2159-8290
 42. Righi E, Kashiwagi S, Yuan J, Santosuosso M, Leblanc P, Ingraham R, et al. CXCL12/CXCR4 blockade induces multimodal antitumor effects that prolong survival in an immunocompetent mouse model of ovarian cancer. *Cancer Res* (2011) 71:5522–34. doi: 10.1158/0008-5472.CAN-10-3143
 43. Feig C, Jones JO, Kraman M, Wells RJ, Deonarine A, Chan DS, et al. Targeting CXCL12 from FAP-expressing carcinoma-associated fibroblasts synergizes with anti-PD-L1 immunotherapy in pancreatic cancer. *Proc Natl Acad Sci U S A* (2013) 110:20212–7. doi: 10.1073/pnas.1320318110
 44. Portella L, Vitale R, De LS, D'Alterio C, Ierano C, Napolitano M, et al. Preclinical development of a novel class of CXCR4 antagonist impairing solid tumors growth and metastases. *PLoS One* (2013) 8:e74548. doi: 10.1371/journal.pone.0074548
 45. Ishiguro T, Ohata H, Sato A, Yamawaki K, Enomoto T, Okamoto K. Tumor-derived spheroids: Relevance to cancer stem cells and clinical applications. *Cancer Sci* (2017) 108:283–9. doi: 10.1111/cas.13155
 46. Quatromoni JG, Eruslanov E. Tumor-associated macrophages: function, phenotype, and link to prognosis in human lung cancer. *Am J Transl Res* (2012) 4:376–89.
 47. Benner B, Scarberry L, Suarez-Kelly LP, Duggan MC, Campbell AR, Smith E, et al. Generation of monocyte-derived tumor-associated macrophages using tumor-conditioned media provides a novel method to study tumor-associated macrophages in vitro. *J Immunother Cancer* (2019) 7:140. doi: 10.1186/s40425-019-0622-0
 48. Kreso A, Dick JE. Evolution of the cancer stem cell model. *Cell Stem Cell* (2014) 14:275–91. doi: 10.1016/j.stem.2014.02.006
 49. Magee JA, Piskounova E, Morrison SJ. Cancer stem cells: impact, heterogeneity, and uncertainty. *Cancer Cell* (2012) 21:283–96. doi: 10.1016/j.ccr.2012.03.003
 50. Sowa T, Menju T, Sonobe M, Nakanishi T, Shikuma K, Imamura N, et al. Association between epithelial-mesenchymal transition and cancer stemness and their effect on the prognosis of lung adenocarcinoma. *Cancer Med* (2015) 4:1853–62. doi: 10.1002/cam4.556
 51. Adorno-Cruz V, Kibria G, Liu X, Doherty M, Junk DJ, Guan D, et al. Cancer stem cells: targeting the roots of cancer, seeds of metastasis, and sources of therapy resistance. *Cancer Res* (2015) 75:924–9. doi: 10.1158/0008-5472.CAN-14-3225
 52. Lorenzo-Sanz L, Munoz P. Tumor-Infiltrating Immunosuppressive Cells in Cancer-Cell Plasticity, Tumor Progression and Therapy Response. *Cancer Microenviron* (2019) 12:119–32. doi: 10.1007/s12307-019-00232-2

53. Maccalli C, Volonte A, Cimminiello C, Parmiani G. Immunology of cancer stem cells in solid tumours. A review. *Eur J Cancer* (2014) 50:649–55. doi: 10.1016/j.ejca.2013.11.014
54. Abdullah LN, Chow EK. Mechanisms of chemoresistance in cancer stem cells. *Clin Transl Med* (2013) 2:3. doi: 10.1186/2001-1326-2-3
55. Dongre A, Weinberg RA. New insights into the mechanisms of epithelial-mesenchymal transition and implications for cancer. *Nat Rev Mol Cell Biol* (2019) 20:69–84. doi: 10.1038/s41580-018-0080-4
56. Dongre A, Rashidian M, Reinhardt F, Bagnato A, Keckesova Z, Ploegh HL, et al. Epithelial-to-Mesenchymal Transition Contributes to Immunosuppression in Breast Carcinomas. *Cancer Res* (2017) 77:3982–9. doi: 10.1158/0008-5472.CAN-16-3292
57. Chen L, Gibbons DL, Goswami S, Cortez MA, Ahn YH, Byers LA, et al. Metastasis is regulated via microRNA-200/ZEB1 axis control of tumour cell PD-L1 expression and intratumoral immunosuppression. *Nat Commun* (2014) 5:5241. doi: 10.1038/ncomms6241
58. Lee Y, Shin JH, Longmire M, Wang H, Kohrt HE, Chang HY, et al. CD44+ Cells in Head and Neck Squamous Cell Carcinoma Suppress T-Cell-Mediated Immunity by Selective Constitutive and Inducible Expression of PD-L1. *Clin Cancer Res* (2016) 22:3571–81. doi: 10.1158/1078-0432.CCR-15-2665
59. Castagnoli L, Cancila V, Cordoba-Romero SL, Faraci S, Talarico G, Belmonte B, et al. WNT signaling modulates PD-L1 expression in the stem cell compartment of triple-negative breast cancer. *Oncogene* (2019) 38:4047–60. doi: 10.1038/s41388-019-0700-2
60. Monteiro I, Vigano S, Faouzi M, Treilleux I, Michielin O, Menetrier-Caux C, et al. CD73 expression and clinical significance in human metastatic melanoma. *Oncotarget* (2018) 9:26659–69. doi: 10.18632/oncotarget.25426
61. Buisseret L, Pommey S, Allard B, Garaud S, Bergeron M, Cousineau I, et al. Clinical significance of CD73 in triple-negative breast cancer: multiplex analysis of a phase III clinical trial. *Ann Oncol* (2018) 29:1056–62. doi: 10.1093/annonc/mdx730
62. Ferrari D, Gambari R, Idzko M, Muller T, Albanesi C, Pastore S, et al. Purinergic signaling in scarring. *FASEB J* (2016) 30:3–12. doi: 10.1096/fj.15-274563
63. Karin N. Chemokines and cancer: new immune checkpoints for cancer therapy. *Curr Opin Immunol* (2018) 51:140–5. doi: 10.1016/j.coi.2018.03.004
64. Di TT, Mazzoleni S, Wang E, Sovena G, Clavenna D, Franzin A, et al. Immunobiological characterization of cancer stem cells isolated from glioblastoma patients. *Clin Cancer Res* (2010) 16:800–13. doi: 10.1158/1078-0432.CCR-09-2730
65. Jinushi M, Baghdadi M, Chiba S, Yoshiyama H. Regulation of cancer stem cell activities by tumor-associated macrophages. *Am J Cancer Res* (2012) 2:529–39.
66. Jung MJ, Rho JK, Kim YM, Jung JE, Jin YB, Ko YG, et al. Upregulation of CXCR4 is functionally crucial for maintenance of stemness in drug-resistant non-small cell lung cancer cells. *Oncogene* (2013) 32:209–21. doi: 10.1038/onc.2012.37
67. Santagata S, Napolitano M, D'Alterio C, Desicato S, Maro SD, Marinelli L, et al. Targeting CXCR4 reverts the suppressive activity of T regulatory cells in renal cancer. *Oncotarget* (2017) 8:77110–20. doi: 10.18632/oncotarget.20363

Conflict of Interest: The authors declare that the research was conducted in the absence of any commercial or financial relationships that could be construed as a potential conflict of interest.

Copyright © 2020 Fortunato, Belisario, Compagno, Giovinazzo, Bracci, Pastorino, Horenstein, Malavasi, Ferracini, Scala, Sozzi, Roz, Roato and Bertolini. This is an open-access article distributed under the terms of the Creative Commons Attribution License (CC BY). The use, distribution or reproduction in other forums is permitted, provided the original author(s) and the copyright owner(s) are credited and that the original publication in this journal is cited, in accordance with accepted academic practice. No use, distribution or reproduction is permitted which does not comply with these terms.